Nuclear Moments of Tb^{157}, Tb^{158}, and Tb^{160} by Electron Paramagnetic Resonance and Nuclear Alignment*

WARREN C. EASLEY,† J. A. BARCLAY, AND D. A. SHIRLEY
Lawrence Radiation Laboratory, University of California, Berkeley, California
(Received 6 November 1967)

Electron-paramagnetic-resonance experiments on yttrium ethylsulfate (YES) single crystals containing terbium isotopes in the relative abundances Tb^{159}:Tb^{157}:Tb^{158}=25:1.6:1 were carried out at Q-band frequencies (35 GHz). The nuclear spin of Tb^{158} was found to be 3, and by comparison with the observed hyperfine structure of Tb^{159} and its known moment, a magnetic moment $\mu^{158}=1.740(7)$ nm was calculated. Transitions due to Tb^{157} were obscured by the stronger Tb^{159} lines. Assuming $I(157)=I(159)=\frac{3}{2}$, the following limits were set on the value of μ^{157}: $\mu^{157}=2.0(1)$ nm. Tb^{160} lines were also observed in YES single crystals. They gave $\mu^{160}=1.685(8)$ nm. Nuclear-alignment experiments on Tb^{158} in a single crystal of neodymium ethylsulfate were also carried out in order to determine a relationship between the quadrupole coupling constant and the magnetic hyperfine structure constant. This information, as well as existing nuclear-orientation results on Tb^{160}, was combined with the EPR data to obtain quadrupole coupling constants. Quadrupole moments calculated from the coupling constants were found to be $Q^{158}=+2.7(5)$ b and $Q^{160}=+3.0(5)$ b.

I. INTRODUCTION

SEVERAL years ago two isotopes of terbium were studied in this laboratory by nuclear orientation in the neodymium ethylsulfate lattice.[1,2] Because of the complexity of the hyperfine structure Hamiltonian relevant to this case, the nuclear-orientation parameters exhibited temperature dependences that were at once unique to terbium ethylsulfate and rather insensitive to the values of the nuclear magnetic moments. The data did, however, yield for each isotope rather accurate functional relationships between the nuclear magnetic dipole and electric quadrupole moments, so that combination of this relationship with an accurate determination of either moment by a different technique would yield the other moment accurately. Supplementary nuclear-orientation measurements yielded approximate values for the individual moments. While neither isotope seemed sufficiently long-lived (Tb^{156}, $t_{1/2}=4$ day and Tb^{160}, $t_{1/2}=72$ day) for electron paramagnetic resonance (EPR) studies, it was thought that both nuclear-orientation and EPR measurements were feasible on Tb^{158} ($t_{1/2}=1200$ yr). These measurements have now been carried out and are reported below. In addition EPR has been observed in Tb^{160}: These data are combined with the earlier orientation results.

II. EXPERIMENTAL

A. Nuclear Alignment of Tb^{158}

The experimental procedures and apparatus for nuclear-orientation studies have been described elsewhere.[1] The Tb^{158} was prepared by neutron irradiation of separated Dy^{156}, via the path $Dy^{156}(n,\gamma)Dy^{157}$ electron capture (EC) $Tb^{157}(n,\gamma)Tb^{158}$. Three microcuries of $^{158}Tb^{3+}$ were grown substitutionally into a 5-g single crystal of neodymium ethylsulfate (NES), which was cooled by adiabatic demagnetization to a series of temperatures in the range $1°K>T>10^{-2}°K$. The warm-up rate of the crystal was monitored with an inductance bridge. Both NaI(Tl) and Ge(Li) detectors were used to measure γ-ray intensities along the crystalline c axis. Heat leaks into the sample were small enough that usually three five-minute cold counts could be taken in succession and the results averaged. Since all five-minute counts agreed within statistical error, inhomogeneous heating effects were shown to be small. Absolute temperatures were determined using the revised NES temperature scale due to Blok *et al.*[3]

B. EPR Measurements

Yttrium ethylsulfate (YES) was chosen as the diamagnetic host for the EPR measurements because it is isostructural to NES. An isostructural salt is required in order to allow the direct comparison of parameters determined in the alignment experiments with those in the EPR experiments.[1,2] Baker and Bleaney[4] have observed the spectrum of natural terbium (100% Tb^{159}, $I=\frac{3}{2}$) in YES and have established the form of the spin Hamiltonian as well as the values of the corresponding parameters.

The amount of Tb^{158} available was small by EPR standards. It was therefore necessary to grow the Tb^{158}: YES single crystal from a very small volume (0.040 cc) of saturated D_2O solution, very slowly (4 weeks), to ensure that the resulting crystal contained most of the activity. The crystal obtained was perfectly formed, weighed approximately 5 mg, and contained 4×10^{14} $^{158}Tb^{3+}$ ions. It was placed in the bottom of a

* Work performed under the auspices of the U. S. Atomic Energy Commission.
† Present address: Department of Chemistry, University of Florida, Gainesville, Fla.
[1] C. E. Johnson, J. F. Schooley, and D. A. Shirley, Phys. Rev. **120**, 2108 (1960).
[2] C. A. Lovejoy and D. A. Shirley, Nucl. Phys. **30**, 452 (1962).
[3] J. Blok, D. A. Shirley, and N. J. Stone, Phys. Rev. **143**, 78 (1966).
[4] J. M. Baker and B. Bleaney, Proc. Roy. Soc. (London) **A245**, 156 (1958).

right circular TE_{011} cavity such that the microwave magnetic field was parallel to the c axis of the crystal.[4] Each of the Tb^{158} and Tb^{160} spectra, in separate samples, was observed at 1°K, using a superheterodyne spectrometer operating near 34.5 GHz with 150-Hz field modulation and synchronous detection. The static magnetic field was measured, using either an NMR gaussmeter (Alpha Scientific-AL67) whose frequency was measured with a Hewlett-Packard 524-B frequency counter, or a rotating coil gaussmeter which had been calibrated with the NMR probe. Mass spectrometric analysis of the terbium sample gave the relative abundances of the three constituents to within an uncertainty of 5%. The results were: Tb^{159}:Tb^{157}:Tb^{158}=25:1.6:1.

The Tb^{160} was prepared by irradiating 0.1 mg samples of natural Tb metal (Research Chemicals, 99.9% pure) for 17 days at a neutron flux of 5.5×10^{14} cm^{-2} sec^{-1} in the MTR reactor, Arco, Idaho. This produced samples containing 2.5% Tb^{160}. Crystals weighing 10 mg and containing approximately 10^{14} $^{160}Tb^{3+}$ ions (0.5 mCi) were grown in a few hours out of 0.4 cc of saturated D_2O solution by rapid evaporation, in order to minimize possible radiation damage effects. It was found, incidentally, that Tb ions tend to grow into ethylsulfate lattice sites much more rapidly than do Y ions. The relatively high paramagnetic ion concentration (nominally 1%) was necessary in order to give sufficient Tb^{160} ions to be observed. However, this concentration also gives an appreciable number of Tb^{159} pairs which also have an EPR spectrum.[5] The pair spectra tended to obscure some of the Tb^{160} lines, but this could not be avoided. For crystals containing 0.5 mCi of activity, no overt radiation damage effects were observed over periods of several hours.

III. FORM OF THE SPIN HAMILTONIAN FOR Tb^{3+} IN ETHYLSULFATE

Tb^{3+} has an electronic configuration [Xe] $4f^8$ and a ground-state term $^7F_6$. (Lande g factor=$\frac{3}{2}$.) In the trigonal field of the ethylsulfate lattice, the term is split into six doublets characterized by $|\pm J_z\rangle$, with the $|\pm6\rangle$ state lowest. The degeneracy of the ground doublet is not complete because of admixing of the $|J_z=0\rangle$ singlet by the sixth-order crystal-field potential V_6^6. The energy levels of the ground-state doublet can be described by the following spin Hamiltonian[1,2,4]:

$$\mathcal{H}=g_{||}\beta HS_z\cos\theta+\Delta_xS_x+\Delta_yS_y+AS_zI_z+P[I_z^2-\tfrac{1}{3}I(I+1)]+cT_z, \quad (1)$$

where $S=\frac{1}{2}$, A is the magnetic hfs constant, P is the quadrupole coupling constant, and θ is the angle between the c axis and the applied field. The normal $\Delta S_z=\pm1$ magnetic dipole transitions have zero probability for the doublet, but transitions of the type $\Delta S_z=0$ are allowed by virtue of the zero-field V_6^6 mixing. The $\Delta S_z=0$ transitions are induced by applying the microwave field parallel to the c axis of the crystal. The zero-field splitting of the doublet is represented by the terms $\Delta_xS_x+\Delta_yS_y$. The term cT_z represents nearest-neighbor dipolar interactions. For Tb^{3+} in NES, $c=-2g_{||}(\mathrm{Tb})g_{||}(\mathrm{Nd})\beta^2/R^3$, where R is the distance to the nearest neighbor. T_z is the projection of the resultant spin of the two nearest neodymium neighbors on the c axis and assumes the values 0, ±1.

The exact energy levels of (1) are given by

$$E(\pm S_z,I_z)=\pm\tfrac{1}{2}[(g_{||}\beta H\cos\theta+AI_z+cT_z)^2+\Delta^2]^{1/2}+P[I_z^2-\tfrac{1}{3}I(I+1)], \quad (2)$$

where $\Delta^2=\Delta_x^2+\Delta_y^2$.

IV. RESULTS

A complete summary of the results of this work is given in Table I. Derivations of the quantities appearing in Table I are discussed in this and the next section.

A. Nuclear Alignment of Tb^{158}

The theory and procedures of obtaining hfs constants from γ-ray anisotropies of Tb isotopes in NES have been discussed previously.[1,2] The appropriate energies levels in zero external field are

$$E(I_z)=-\tfrac{1}{2}[(AI_z+cT_z)^2+\Delta^2]^{1/2}+P[I_z^2-\tfrac{1}{3}I(I+1)]. \quad (3)$$

For a given Tb isotope, only A, P, and sometimes I are unknown. If I is known or a value is assumed on the basis of nuclear systematics, then A and P can be varied until the energy levels in (3) reproduce the experimental nuclear-orientation data. In this way, empirical values of A and P are obtained which can be used to calculate nuclear moments.

The theoretical angular distribution of γ radiation from oriented nuclei is described by the expression[6]

$$W(\theta)=1+B_2U_2F_2P_2(\cos\theta)\cdots$$

plus higher-order terms which were found to be negligible for this experiment. B_2 is an alignment parameter containing all the temperature dependence while U_2 and F_2 are angular momentum factors for the radiations.

TABLE I. Hyperfine structure constants and nuclear moments of tripositive Tb^{157}, Tb^{158}, Tb^{159}, and Tb^{160} in yttrium ethylsulfate.

	Tb^{157}	Tb^{158}	Tb^{159}	Tb^{160}
I	($\frac{3}{2}$)	3	$\frac{3}{2}$	3
A(10^{-4} cm^{-1})	2090(120)	912(9)	2090(20)	883(8)
P(10^{-4} cm^{-1})		48(5)		55(5)
μ(nm)	2.0(1)	1.740(7)	1.994(4)	1.685(8)
Q(barns)		2.7 (5)		3.0 (5)

[5] J. M. Baker and A. E. Mau, Can. J. Phys. 45, 403 (1967).

[6] R. J. Blin-Stoyle and M. A. Grace, in *Handbuch der Physik*, edited by S. Flugge (Springer-Verlag, Berlin, 1957), Vol. XLII, p. 555.

The portion of the decay scheme of Tb^{158} relevant to this work is reproduced in Fig. 1.[7] Although the 946-keV γ ray showed the largest anisotropy (32% at $1/T=90$), we studied the temperature dependence of B_2 through the 182-keV γ ray, using 3 in.×3 in. NaI(Tl) scintillation crystals in order to enhance statistical accuracy. Unambiguous calculation of U_2 for the 182-keV γ ray was not possible, so $U_2(182)$ was obtained by comparison of the angular distribution coefficients of the 946- and 182-keV γ rays, using a Ge(Li) detector. We found

$$\frac{[W(0)-1]_{946}}{[W(0)-1]_{182}}=\frac{U_2(946)F_2(946)}{U_2(182)F_2(182)}=1.025(20).$$

Since $U_2(946)=0.829$, $F_2(946)=-0.418$, and $F_2(182)=-0.448$, we thus have $U_2(182)=+0.757(15)$. A plot

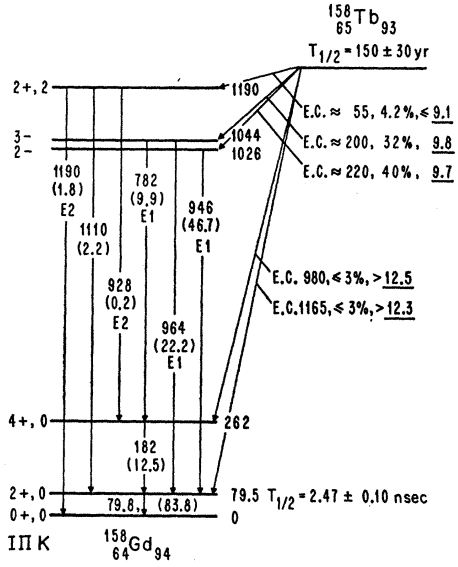

FIG. 1. Portion of Tb^{158} decay scheme relevant to this work.

of the empirical B_2 values determined from $W(0)$ is shown in Fig. 2, with statistical errors indicated. The solid and dashed curves are theoretical fits to the data for the indicated values of $|A|$ and P, with $I(158)=3$. The plot suggests that the true values lay within the broad limits $0.0607<|A|<0.103$ cm^{-1} and $0.00195<P<0.00602$ cm^{-1}. The data are insensitive to the sign of $|A|$, but give an unambiguous determination of the sign of P.[1,2] The most accurate result derived from the data was the following relation between $|A|$ and P:

$$P(158)=0.0985(20)|A(158)|-0.00418(30), \quad (4)$$

in units of cm^{-1}.

[7] F. Schima, E. G. Funk, Jr., and J. W. Mihelich, Nucl. Phys. 63, 305 (1965).

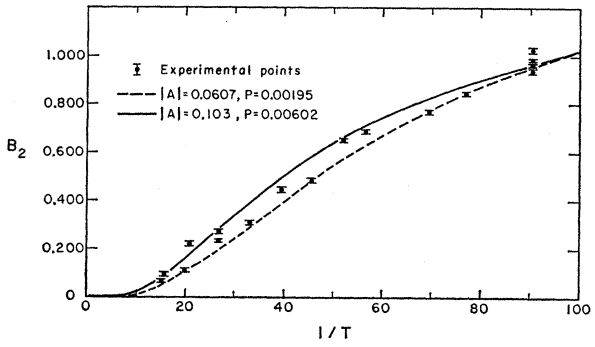

FIG. 2. Experimental and theoretical values of B_2 versus $1/T$ for the 182-keV γ ray of Tb^{158} with the NaI(Tl) detectors parallel to the c axis of the neodymium ethylsulfate crystal.

B. Correction of Tb^{160} Nuclear-Orientation Results

The temperature scale used by Johnson *et al.*[1] to interpret the Tb^{160} nuclear-orientation results has been shown to be in error.[3] We have redetermined the relationship given between $|A|$ and P using the new temperature scale. We find

$$P(160)=0.100(2)|A(160)|-0.00334(20), \quad (5)$$

also in units of cm^{-1}.

C. EPR of Tb^{157}, Tb^{158}, Tb^{160}

The energy levels of dilute Tb^{3+} in YES are obtained from Eq. (2) by setting cT_z equal to zero. The energies of the allowed $\Delta I_z=0$ transitions are then

$$h\nu=[(g_{||}\beta H\cos\theta+AI_z)^2+\Delta^2]^{1/2}. \quad (6)$$

Note that the quadrupolar term vanishes for the allowed transitions, showing that the EPR frequencies are completely insensitive to P. For Tb^{159}, Baker and Bleaney give[4] $g_{||}=17.72(2)$, $\Delta=0.387$ cm^{-1}, and $|A|=0.209(2)$ cm^{-1}. The magnetic fields at resonance are found by solving Eq. (6) for H:

$$H=\frac{[(h\nu)^2-\Delta^2]^{1/2}-AI_z}{g_{||}\beta\cos\theta}.$$

The spacing ΔH between two adjacent hyperfine lines I_z and I_z+1 is then just

$$\Delta H=H(I_z)-H(I_z+1)=A/(g_{||}\beta\cos\theta).$$

Thus the spacings between hyperfine components are equal and are directly proportional to the hyperfine structure constant. This allows the determination of A by direct comparison of observed splittings between the radioactive isotopes and stable Tb^{159}. The accuracy in A is limited by the uncertainty in A^{159}, i.e., ±1%. However, it is possible to obtain much more accurate magnetic moment values from the observed splittings, as will be discussed in Sec. V.

1. Tb^{157}, Tb^{158}

The $Tb^{158,159}$($Tb^{159}/Tb^{158}=25$) EPR spectrum consisted of four strong lines due to Tb^{159} single-ion transitions superimposed upon the weaker Tb^{158} seven-line spectrum. In Fig. 3 a portion of the spectrum is reproduced, with the positions of three of the Tb^{158} lines indicated by vertical arrows, including the center line. Five of the seven Tb^{158} lines were completely resolved, including the two outermost at either end of the spectrum, and the nuclear spin of 3 was confirmed. Two of the lines were particularly obscured by the strong Tb^{159} single-ion absorptions, as shown in Fig. 3. Table II gives the line positions for $\theta=0$ and the measured hf splittings. The satellite structure about the Tb^{159} lines, designated A, B, and C in Fig. 3, is due to distant-neighbor Tb^{159} pairs. The details of the pair spectrum are discussed below. The positions of the pair lines have been omitted from Table II. Using the values of ΔH given in Table II we calculate $|A(158)|=0.0912(9)$ cm^{-1}. This value agrees with the results of the nuclear-alignment experiment. Using $|A(158)|$ in Eq. (4), we find $P(158)=0.0048(5)$ cm^{-1}.

Mass-spectrometer analysis of the sample yielded the ratio $Tb^{157}/Tb^{158}=1.6(1)$. If Tb^{157} has the same nuclear spin as Tb^{159} ($\frac{3}{2}$), as expected, then each of the four Tb^{157} lines should be $1.6\times7/4=2.7$ times as intense as a Tb^{158} line. We did not observe any transitions of this intensity in the EPR spectrum. This was expected because the magnetic moment of Tb^{157} probably arises from a $\frac{3}{2}+[411]$ proton orbital—the same orbital responsible for the Tb^{159} moment. Hence, we conclude that the Tb^{157} transitions are buried beneath the stronger ($Tb^{159}/Tb^{157}=16$) Tb^{159} lines. By determining where lines of the expected intensity would start to affect the Tb^{159} line shape, we can set limits on $A(157)$. Of course, this analysis is complicated by the presence of the two partially resolved transitions belonging to the pair doublets "C," which lie at approximately ±12 G about each main hf component. Thus, to be safe, we conclude that the Tb^{157} lines must be within ±15 G of the Tb^{159} lines. This gives

$$|A(157)|=0.21\pm0.01 \text{ cm}^{-1}.$$

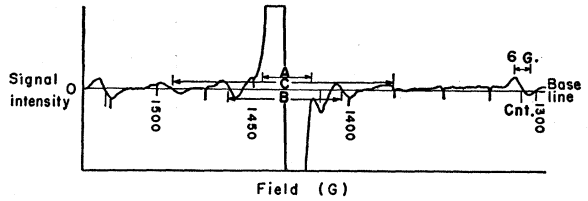

FIG. 3. Portion of the Q-band EPR spectrum of $Tb^{158,159}$ in yttrium ethylsulfate at 1°K. The vertical arrows mark the positions of 3 of the Tb^{158} lines, including the line at centroid of the spectrum. The satellite structures A, B, and C about the strong Tb^{159} single-ion transition are due to Tb^{159} pairs.

2. Tb^{160}

Figure 4 shows the same portion of the $Tb^{160,159}$ spectrum as shown for $Tb^{158,159}$ in Fig. 3 and Table III gives the corresponding line positions and Δh's. The linewidths are approximately twice those in Fig. 3 due to radiation damage effects and/or imperfections in the crystal caused by rapid growth. This increase in linewidth prevented us from observing four of the seven Tb^{160} lines due to overlap of either the Tb^{159} single-ion or pair lines. However, since the nuclear spin of Tb^{160} has been conclusively established[1,8,9] as 3, we are confident in the assignment of the following hfs constant based on the positions of the three observed lines: $|A(160)|=0.0883(8)$ cm^{-1}. Verification that the three observed lines are due to Tb^{160} was obtained by examining "cold" Tb^{159}:YES crystals which had been grown in exactly the same way as the radioactive crystals. The three lines assigned to Tb^{160} were absent from the EPR spectra of those crystals.

Using Eq. (5), we find $P(160)=0.0055(5)$ cm^{-1}.

TABLE II. $Tb^{158,159}$ EPR line positions in yttrium ethylsulfate. $\nu\cong34.5$ GHz. The values are averages of "up" and "down" field sweeps.

Tb^{158}(G)	Tb^{159}(G)
	930.2
978.2	
1088.4	
	1182.2
...	
1308.5 (center)	
...	
	1434.7
1528.6	
1638.1	
	1686.6
ΔH^{158}(av) = 110.0(3)	
ΔH^{159}(av) = 252.1(3)	

3. Pair Spectra

A satellite structure composed of three pairs of lines, designated A, B, and C in Figs. 3 and 4, was observed about *each* of the four Tb^{159} hf lines. The lines were nearly symmetrically displaced about the main lines with total splittings which varied somewhat from one hf component to the next. The total splittings about the high-field hf component were 124 G for A, 61 G for B, and approximately 25 G for C, as measured with H parallel to the c axis. The splittings decreased at lower fields, with values of 111 G, 55 G, and 23 G, for A, B, and C, respectively, about the lowest-field hf component. We have assigned this structure to dipolar-coupled pair transitions.

[8] H. Postma and W. J. Huiskamp, in *Proceedings of the Seventh International Conference on Low-Temperature Physics, 1960*, edited by G. M. Graham and A. C. Hollis (University of Toronto Press, Toronto, 1960), p. 180.

[9] A. Y. Cabezas, I. Lindgren, and R. Marrus, Phys. Rev. **122**, 1796 (1961).

At the higher paramagnetic-ion concentrations (nominally 1%), an appreciable number of paramagnetic-ion pairs exist in the crystal. An approximate spin Hamiltonian describing such a pair is just the sum of the two single-ion spin Hamiltonians plus the dipolar interaction. For the special case of two identical ions, 1 and 2, lying along the c axis and separated by a distance R, the interaction term can be written $aS_{1z}S_{2z}$, where $a=-2g_{||}^2\beta^2/R^3$. The general form of the dipolar interaction is more involved, depending in a complicated way on the angular variables as well. Baker and Mau[4] have calculated the energy levels corresponding to the two *nearest*-neighbor Tb ions which are separated by 7 Å along c. At magnetic fields corresponding to 35 GHz, they found a spectrum composed of many lines (because the states are thoroughly mixed by the large dipolar interaction). Although some of these lines lie between the main hfs lines we did not observe them, presumably because their intensities were too low. (These nearest-neighbor lines are at least 3 to 4 times less intense than those of the other pairs, as will be shown below.)

TABLE III. $Tb^{160,159}$ EPR line positions in yttrium ethylsulfate. $\nu\cong 34.1$ GHz. The values are averages of "up" and "down" field sweeps.

Tb^{160}(G)	Tb^{159}(G)
	923.7
...	
1092.8	
	1176.2
...	
1307.3 (center)	
...	
	1434.7
1520.8	
...	
	1686.6
ΔH^{160}(av) = 107.0(5)	
ΔH^{159}(av) = 253.2(8)	

The interaction between more distant pairs, which is much smaller, results in a single spectrum of two lines, one on either side of the single-ion lines for each central ion-distant neighbor pair.[4] The exact positions of the lines are obtained by solving the complete energy matrix problem. However, the spacings between the lines of each doublet are, to first order, just twice the dipolar field generated by the distant neighbor. The component of the dipolar field along the c axis due to a Tb ion at a point (R,θ,ϕ), where the polar axis is taken as the c axis with the origin at the central ion, can be written

$$H_c=H_d\cos\xi,$$

where

$$H_d=g_{||}(\mathrm{Tb})\beta S_z[4\cos^2\theta+\sin^2\theta]^{1/2}/R^3$$

and

$$\xi=[\theta+\tan^{-1}(\tfrac{1}{2}\tan\theta)].$$

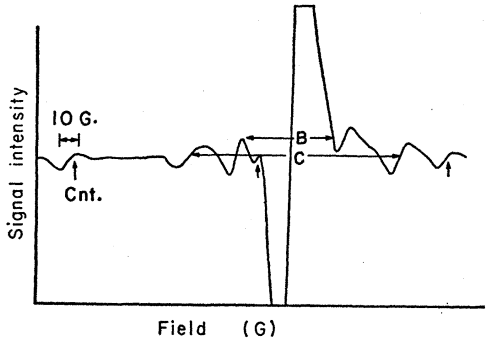

FIG. 4. Portion of Q-band EPR spectrum of $Tb^{160,159}$ in yttrium ethylsulfate at 1°K. The vertical arrows indicate the positions of three of the Tb^{160} lines, including the line at the centroid of the spectrum. The doublet A is not resolved from the Tb^{159} single-ion transition.

Using the x-ray data of Fitzwater and Randle[10] on YES, and allowing for an isotropic 1% contraction of the lattice parameters due to the temperature difference between their measurements and ours, we may calculate dipolar fields due to various neighbors. The results are summarized in Table IV. The contributions are seen to fall into three groups with splittings which correspond quite well with the observed splittings A, B, and C. The first-order approximation is best at the high-field transition because then $g_{||}\beta H$ is sufficiently larger than the dipolar perturbation. The expected relative intensities are roughly 4 to 6 to 9, which are in accord with the observed intensities. Hence we may attribute the satellite structure observed about the single-ion hf transitions to dipolar-coupled pairs.

V. CALCULATION OF NUCLEAR MOMENTS

The magnetic hfs constant A is related to the measured spacing between the hf components by the equation $|A|=k\Delta H$, where $k=(g_{||}\beta\cos\theta)^{-1}$ is constant for all the Tb isotopes within a given crystal. Hence the nuclear magnetic moments of Tb^{158} and Tb^{160} can be accurately calculated from the EPR results, using the equation

$$\mu^{158,160}=\frac{\mu^{159}\Delta H^{158,160}I(158,160)}{\Delta H^{159}I(159)},$$

TABLE IV. Components of the dipolar fields along the c axis at the central Tb ion due to surrounding neighbors.

Pair	No. of sites	R(Å)	θ	H_c(G)
	2	7.00	0	479
C	6	8.71	66°24′	64.6
B	6	13.2	37°12′	32.2
B	6	13.8	90°	31.2
C	2	14.0	0	58.3
A	12	15.4	66°24′	12.0
A	6	19.2	24°29′	16.6
A	2	21.0	0	17.6

[10] D. R. Fitzwater and R. E. Rundle, Z. Krist. 112, 362 (1959).

which eliminates the dependence of the determination on θ and the other parameters in the spin Hamiltonian. The ΔH values are given in Tables II and III. μ^{159} has been determined from ENDOR measurements as $+1.994(4)$ nm.[11] This method neglects any possible hyperfine anomaly.[12,13] Because most of the moment in the odd-odd isotopes arises from the same proton orbital as in Tb^{159}, $\frac{3}{2}+[411]$, the anomaly should be much smaller than the experimental errors. The results are $|\mu^{158}|=1.740(7)$nm and $|\mu^{160}|=1.685(8)$nm.

From the limits set on $A(157)$ we also find

$$\mu^{157}=2.0(1)\text{nm}.$$

The nuclear electric quadrupole moments Q can be calculated from the expression[14]

$$P=P_{\text{lattice}}+P_{4f}=Q\Big[-\frac{3}{I(2I-1)}\times(1-\gamma_\infty)A_2{}^0 - \frac{3e^2}{4I(2I-1)}\times(1-R_Q)\langle r^{-3}\rangle_{4f} \times\langle 3J_z{}^2-J(J+1)\rangle\langle J\|\alpha\|J\rangle\Big].$$

Here $(1-\gamma_\infty)A_2{}^0$ is the antishielded crystal field gradient, R_Q is the "atomic Sternheimer factor," $\langle r^{-3}\rangle_{4f}$ is the *actual* expectation value of r^{-3} for the $4f$ shell, and $\langle J\|\alpha\|J\rangle$ is a reduced matrix element. The following values were used for the calculation

$$(1-\gamma_\infty)A_2{}^0=3.5(5)\times10^4\ \text{cm}^{-1}\ a_0{}^{-2}\ \text{(Ref. 11)},$$
$$(1-R_Q)\langle r^{-3}\rangle_{4f}=8.23\ \text{a.u. (Ref. 8)},$$
$$\langle 3J_z{}^2-J(J+1)\rangle=(104.7-42.0)\ \text{(Ref. 3)},$$
$$\langle J\|\alpha\|J\rangle=-1/99\ \text{(Ref. 12)}.$$

Using these values together with the values for $P(158)$ and $P(160)$ obtained from the alignment and EPR measurements, we find $P=[0.00180(40)\ \text{cm}^{-1}/\text{b}]Q$, which gives $Q(158)=2.7(5)$ b and $Q(160)=3.0(5)$ b.

VI. DISCUSSION

The odd proton and odd neutron in Tb^{158} and Tb^{160} occupy $\frac{3}{2}+[411]$ and $\frac{3}{2}-[521]$ states, respectively.[15] Theoretical calculations of magnetic moments, using Nilsson wave functions (with $\eta=+6$), have been carried out previously, yielding $+2.0$ nm.[1,2] It is interesting to note that, using the magnetic moment of the $\frac{3}{2}+[411]$ proton state of Tb^{159}($+1.994$ nm) and the average moment of the $\frac{3}{2}-[521]$ states of Gd^{155} and Gd^{157} (-0.283 nm),[16] and neglecting odd-particle correlations, one obtains a moment of $+1.711$ nm, in excellent agreement with the magnitudes of the experimental values. Hence, we can assign positive signs to both A and μ for Tb^{158} and Tb^{160}. The signs of the parameters listed in Table I correspond to this assignment.

From the relation[16] $Q=Q_0(I/I+1)(2I-1/2I+3)$, we may calculate intrinsic quadrupole moments $Q_0(158)=6.5\pm1.2$ b and $Q_0=7.2\pm1.2$ b, in excellent agreement with those of other nuclei in this region.

ACKNOWLEDGMENTS

We gratefully acknowledge the assistance of the following people in this work: Dr. J. M. Baker of the Clarendon Laboratory, Oxford University, for suggesting the origin of the satellite structure; Dr. Maynard Michel of the LRL for performing the mass spectrometer analysis of the $Tb^{157,158,159}$ sample; and Mrs. Winifred Heppler for assisting in the sample preparation.

[11] J. M. Baker, J. R. Chadwick, G. Garton, and J. P. Hurrell, Proc. Roy. Soc. (London) **A286**, 352 (1965).
[12] J. Eisinger and V. Jaccarino, Rev. Mod. Phys. **30**, 528 (1958).
[13] B. Bleaney, *Quantum Electronics 3* (Columbia University Press, New York, 1964), p. 595.
[14] J. Blok and D. A. Shirley, Phys. Rev. **143**, 278 (1966).
[15] S. G. Nilsson, Kgl. Danske Videnskab. Selskab, Mat. Fys. Medd. **29**, No. 16 (1955).
[16] I. Lindgren, in *Alpha-, Beta-, and Gamma-Ray Spectroscopy*, edited by K. Siegbahn (North-Holland Publishing Co., Amsterdam, 1964).